OPTIMIZATION OF CONTROL PARAMETERS IN A FRICTION HYDRO PILLAR PROCESSING UNIT TO REPAIR OIL STEEL STRUCTURES

Gabriela Mendes Santos, gmsgabriela@gmail.com
Camila Monteiro Formoso, camilaformoso@yahoo.com.br
Sinésio Domingues Franco, sdfranco@ufu.br
Vera Lúcia Donizeti de Souza Franco, vlfranco@ufu.br
School of Mechanical Engineering, Federal University of Uberlândia, Avenida João Naves de Ávila, 2121, Bairro Santa Mônica, Uberlândia – MG, Brasil

Abstract. *Offshore repair of steel structures in the oil industry represents high financial costs. It is even worse since these operations are carried out in explosion risk areas. In these cases, to repair cracks or other structure defects the most used technique is the underwater arc welding. However, it has some disadvantages, such as: hyperbaric welding, need of drydock structure, welding bead porosity, material embrittlement due to hydrogen adsorption and formation of brittle phases. An alternative to the arc welding is the friction hydro pillar processing (FHPP), where a hole is drilled at the damaged area and filled with a consumable rod of the same material. The rod is rotated and pressed against the hole, leading to frictional heating and, as a consequence, the rod material flows along its shear planes and fills the hole. This repair process occurs below the melting point of the base and consumable materials, so that the problems observed during the arc welding does not appear. Looking forward to applying this technology, a portable FHPP equipment was designed and built to carry out this process. To automate the machine, a software was developed, using the software LabView®, version 8.5. The main controlled and monitored process parameters were: rod rotation, axial force and burn-off length. Additionally, the shaft torque is measured. This work presents the details of the rotation control tuning, that is directly related to the width of the heating affected zone (HAZ). In order to tune the rotation speed, a PID algorithm was chosen due to its simplicity. In this case, it was necessary to identify the equipment closed loop circuit, data acquisition boards, transference function, control tuning method and values P, I and D. Tests performed with the developed PID algorithm demonstrated its effectiveness on tuning the rotation.*

Keywords*: friction hydro pillar processing, optimization, control tuning*

1. INTRODUCTION

Equipment maintenance in the oil industry is not an easy operation. As a substitute method to repair steel structures in this industry sector, a process called Friction Hydro Pillar Processing (FHPP) has been proposed to substitute the conventional technique of underwater electric-arc welding that may lead to many inconvenient such as porosity and gas adsorption (Andrews, 1990; Thomas and Nicholas, 1992, Nicholas, 1995 and Thomas and Tempel-Smith, 1997).

The FHPP process consists of making a cylindrical or tapered hole in the defect region and filling it with a pin of the same geometry, subjected to high speeds and axial forces, as shown in Fig. 1. Due to friction between the pin and hole surface, there is an increase in temperature of contact surfaces, leading to a reduction in yield strength, favoring thus the plastic flow of pin and base materials (Meyer, 2002).

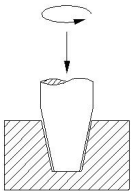

Figure 1. Pin and hole geometries used in the FHPP technique (Hwang, 2010).

In order to apply the FHPP in the field, it was proposed to build a portable Friction Hydro Pillar Processing Unit, in Portuguese, *Unidade de Processamento de Pinos por Atrito* (UPPA), by the Laboratory of Friction and Wear Technology at the School of Mechanical Engineering, Federal University of Uberlandia. This equipment should be able to perform tests with speeds up to 5,000 rpm and axial forces up to 40 kN (Hwang, 2010).

To achieve the automation and data acquisition and monitoring of this unit, a program was developed using LabView® (Santos *et al*, 2010). This program is responsible for graphic display and storage of parameters, such as rotational speed, axial force, torque and burn-of-length during the test. These parameters are controlled by a PID controller card that keeps the axial force and rotation close to the set values. This work is focused on the optimization of rotation control.

2. OBJECTIVES

The objective of this work is to optimize P, I and D variables of a controller card used in a portable Friction Hydro Pillar Processing Unit, so that the pin rotation can be better controlled during the process. This optimization is achieved through the identification of closed loop control behavior, study of data from already carried out tests and system transfer function. Thus, using an appropriate control method, it is possible to calculate the optimal variable values of rotation controller card. Finally, the control tuning is verified in laboratory tests.

3. METHODOLOGY

To achieve the objectives of this work, first of all, it is necessary to describe the processing unit and its components. Furthermore, an analysis of acquired and stored data is presented to obtain the system transfer function. Thus, from a chosen tuning method, the variables P, I and D of the rotation control card can be calculated.

3.1. Closed loop identification

The UPPA unit can be divided into two subsystems that are the mechanical and the electrical one. The mechanical system consists of a hydraulic unit that is responsible for the hydraulic flow to the welding head. The welding head is driven by a hydraulic motor, that it is able to rotate the pin with a rotation speed of up to 5,000 rpm. This motor is mounted on a hydraulic cylinder that can push the pin against the hole with an axial force of up to 40 kN.

The electrical subsystem is responsible for driving the electrical motors and data acquisition during the tests. There are basically power and control elements, such as electric motors, servo valves, sensors and an electrical panel. This panel contains elements which are part of UPPA's control loop, as for instance a Programmable Logic Controller (PLC), PID controller cards and electronic circuits of the sensors involved in (Souza, 2006).

To accomplish the equipment's automation, it was developed a program using the software LabView®, version 8.5, to send control parameters as well as to acquire and store signals, such as: rotation speed, axial force, torque and burn-of-length.

This communication was carried out with the aid of a data acquisition board PCI-DAS 1200, AD / DA, 12 bit resolution, 330 kHz, from Measurement Computing Corporation. The analog ports operate at -10 to +10V (DC) voltage rage and the digital ones operate at TTL level of 0 to +5V. In addition, sensors were added to monitor pressure, position and rotation. In order to acquire the rotation signal, an inductive sensor was used that operates according to the reluctance principle. To measure this variable, a metallic knuckle wheel was attached to the welding head and a sensor placed close to it (about 2mm). In this case, the maximum output signal was 15V that corresponds to the same value of the supply voltage. The lower output signal was 0V, corresponding to a distance far greater than 2mm between the wheel and the sensor. However, the so generated signal, that has a square wave form, is incompatible with the data acquisition board. This board offers no option for a digital signal input. So, to make the rotation sensor signal compatible with the data acquisition board, it was necessary to build an analog circuit capable of converting a square wave into a continuous analog voltage. The output voltage of this circuit is limited to a maximum of 9V to protect the system against damages (Formoso *et al.*, 2005).

The VT-HACD card is responsible for the rotation control, according to the values set by the operator. The setpoint is given via a man machine interface, whose value is passed to the PLC. After entering the data, it is possible to perform the closed loop process, maintaining the acquired signal close to the reference. With this, the card sends signals to open and to close a valve, which is responsible for sending oil to a hydraulic motor, as shown in Fig. 2. So, the rotation control is achieved during the tests and it is also monitored through the program aforementioned.

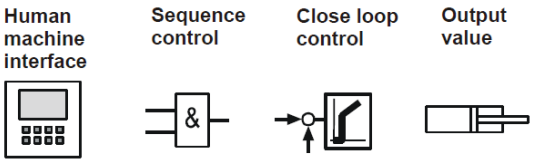

Figure 2. Control valve sequence (Rexroth Bosch Group, 2007).

The controller card structure itself has the PIDT-1 form, in which every component can be individually enabled or disabled. This behavior has proportionally - integrative - derivative with low pass filter forms. It allows also the P or PT-1 behavior. The first corresponds to the proportional controller and the latter to proportional and low pass filter. Figure 3 shows the controller block diagram.

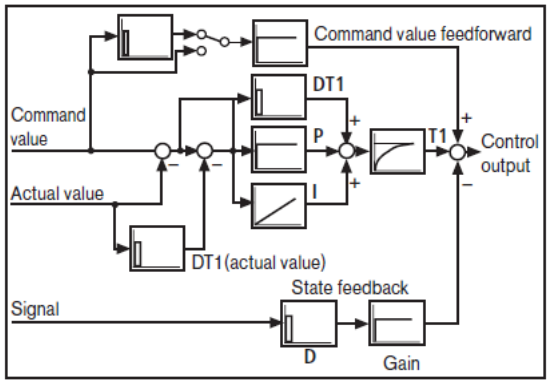

Figure 3. Controller block diagram (Rexroth Bosch Group, 2007).

The output control signal is resulted from a combination between the command value (setpoint) and the feedback action.

3.2. Transfer function identification

In order to achieve the system transfer function, data stored by the monitoring program were analyzed. Figure 4 displays test 1 graphical signals of rotation, axial force and burn-of-length. The desired rotation setpoint is 5,000 rpm. This figure shows a sharp reduction on the rotation value associated with a force peak. After about seven seconds, the system lost the stability and stalled.

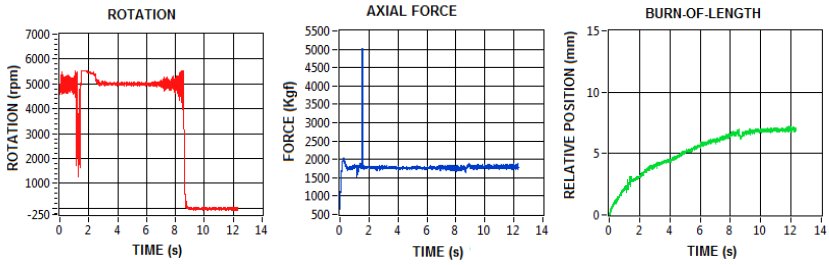

Figure 4. Graphical signals with rotation setpoint 5,000 rpm, axial force of 1,750 kgf and 13mm burn-of-length.

Figure 5 shows test 2 graphical signals of rotation, axial force and burn-of-length. The rotation setpoint value was 5,000 rpm. At the beginning of the test, close to 1s of test duration, the system suffers from instability and the fall in the value of rotation, while a peak of 5,000 kgf of axial force is observed. Subsequently, the control tries to be achieved, as can be seen from the chart at 3s, despite the existing oscillation. However, in spite of this attempt, there are large variations, which lead to a locking of the equipment.

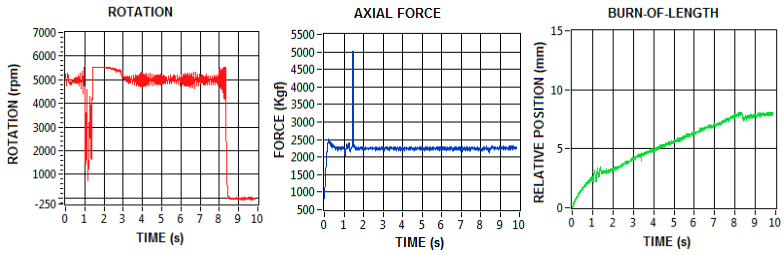

Figure 5. Graphical signals with rotation setpoint 5,000 rpm, axial force 1,750 kgf and 13mm burn-of-length.

Figure 6 presents test 3 graphical signals of rotation, axial force and burn-of-length. In the rotation graphical signal, it can be seen that the system behaves in a stable way, presenting small oscillations. The expected value of 5,000 rpm is achieved, however, the force increases and the rotation stops. This shows the locking of the system, evidenced by the short burn-of-length, less than 5mm.

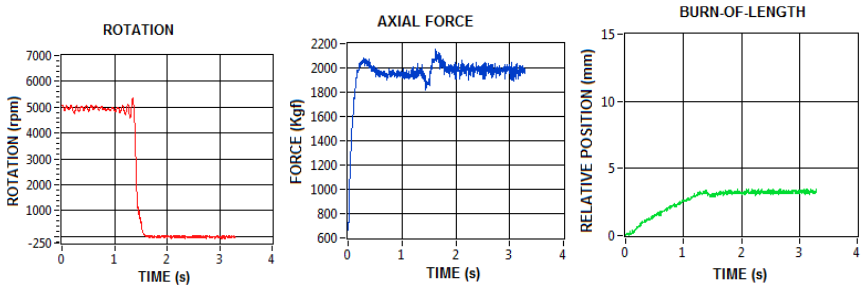

Figure 6. Graphical signals with rotation setpoint 5,000 rpm, axial force 2,000 kgf and 13mm burn-of-length.

Figure 7 shows the test 4 graphical signals of the rotation, axial force and burn-of-length. This Figure also shows that the card works in closed loop control, however, only to check minimum and maximum limits. There is only a step input with setpoint of 5,500 rpm and some noise. With this configuration, the axial force reached the set value of 2,200 kgf and the 13mm burn-of-length.

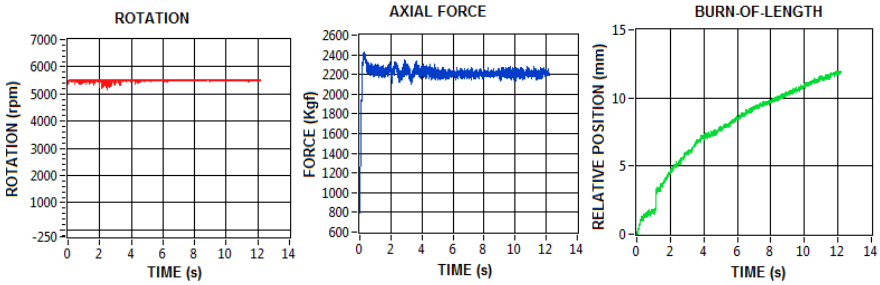

Figure 7. Graphical signals with rotation setpoint 5,500 rpm, load of 2,200 kgf and 13mm burn-of-length.

In order to accomplish the identification of PID parameters, it was necessary to obtain the system transfer function. For this, a test was performed with reference values (setpoint) and reading the response of the rotation (feedback) in voltage from 0 to 10V. The input values were varied in steps and the result can be seen from Fig. 8 that shows no random noise. Moreover, it can be mentioned that there is more input value fluctuations below 2V and above 4V, which shows possible limitations of the system.

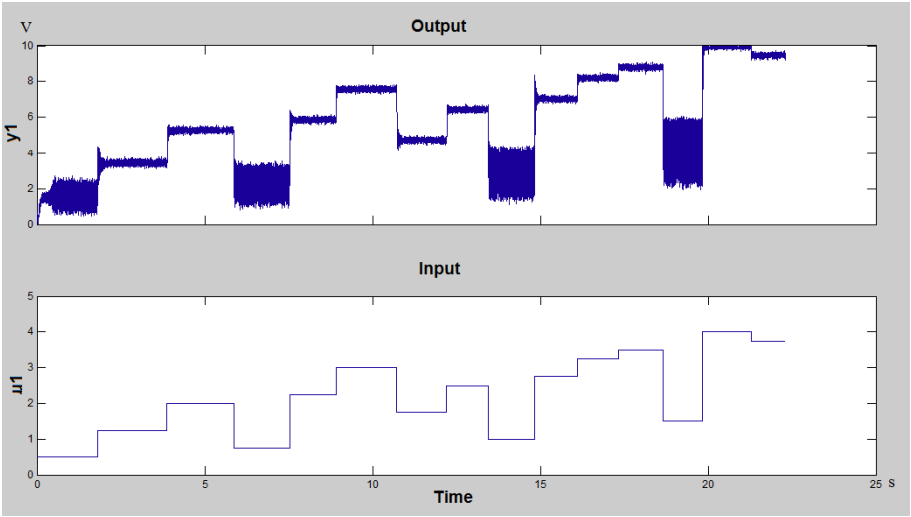

Figure 8. System response varying values in tension.

This result is consistent with the operation of used valve in FHHP equipment; this has a limited action. For above 5V and below 2V it is unable to control the oil flow to the hydraulic motor. Thus, there is the possible to find the operation range of equipment. Under these conditions, input values between 2V and 4V from test 2 were chosen to perform the evaluation of the transfer function.

Figure 9 shows the data chosen to find the transfer function.

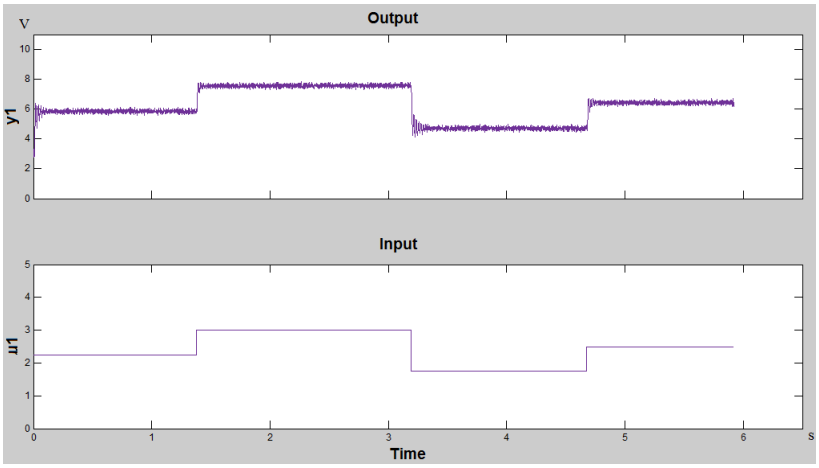

Figure 9. Chosen data to identify the transfer function.

Using the toolkit "ident" of the Matlab® software, as shown in Fig. 10, test data and reference function (the desired setpoint value) have to be given to "Import data" field. The first is positioned in Working Data, while the second is allocated in Validation Data Compiling. Then, it is possible to estimate the transfer function through the function Estimate. From the option "Process models" in "Estimate" function, the curves were obtained, that can be seen in Fig. 11.

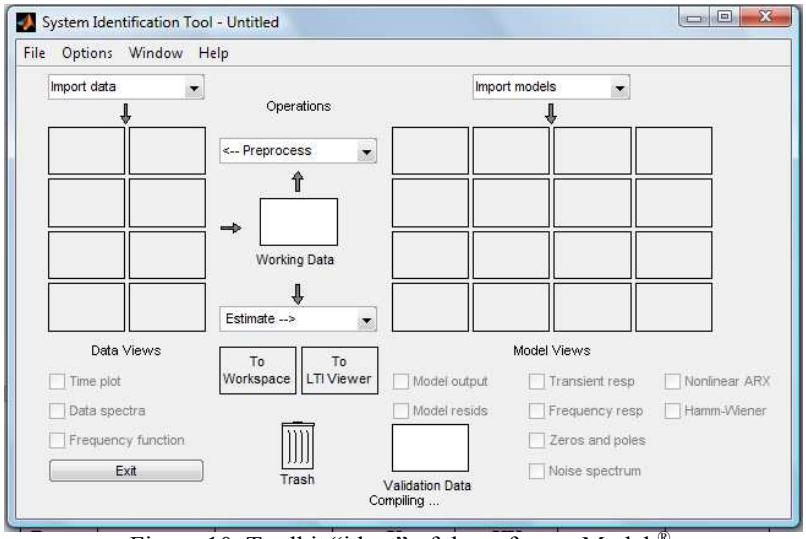

Figure 10. Toolkit "ident" of the software Matlab®.

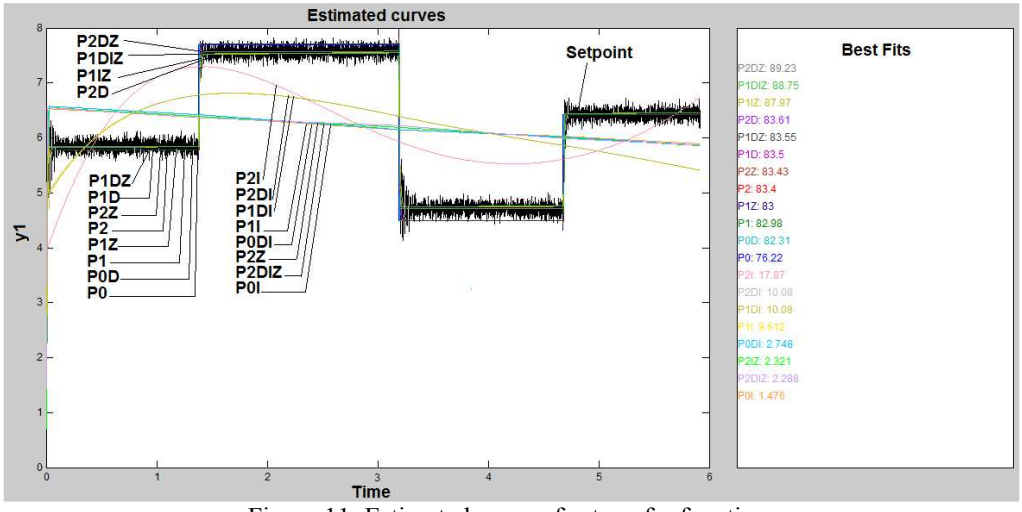

Figure 11. Estimated curves for transfer function.

It can be seen from Fig. 11 that the best approaches are: P2DZ, P1DIZ and P1IZ. They present best fit close to 90%, values that seems to be consistent with criteria analyzed to choose the transfer function of the system. In this case, the P1IZ was chosen, because this term has no delay. With the system transfer function, it is possible to calculate the controller PID parameters.

3.3. Tuning control

Before explaining the technique used to calculate the proposed control parameters, some comments on the PID controller should be mentioned. This is probably the most widely used controller in control systems in negative feedback cases due to its simplicity, good dynamic properties and robustness (Paula *et al.*, 2010). A standard notation is shown by Eq. 1,

$$K(s) = K_P\left(1 + \frac{1}{T_I s} + T_D s\right) \tag{1}$$

where KP is the proportional gain, TI the integral action time and TD the time derivative action.

The technique of tuning controllers by analytical frequency response was chosen. In this, gain and phase margins are measures of stability for a feedback system, though often times only phase margin is used rather than both. Based on the magnitude response of the loop gain, $|A_{OL}b|$, gain margin is the difference between unity and $|A_{OL}b(\omega_{180°})|$ where $\omega 180°$ is the frequency at which the loop gain phase, $|A_{OL}b|$, is -180°. Phase margin is the phase difference between $|A_{OL}b(\omega_0 dB)|$ and -180° where ω_0 dB is the frequency at which $|A_{OL}b|$ is unity. Gain and phase margins are illustrated below in Fig. 12. Note that a target phase margin of 60° is highly desirable in feedback amplifier design as a tradeoff between loop stability and settling time in the transient response. Typically, the minimum acceptable phase margin is 45° (Blalock, 2001).

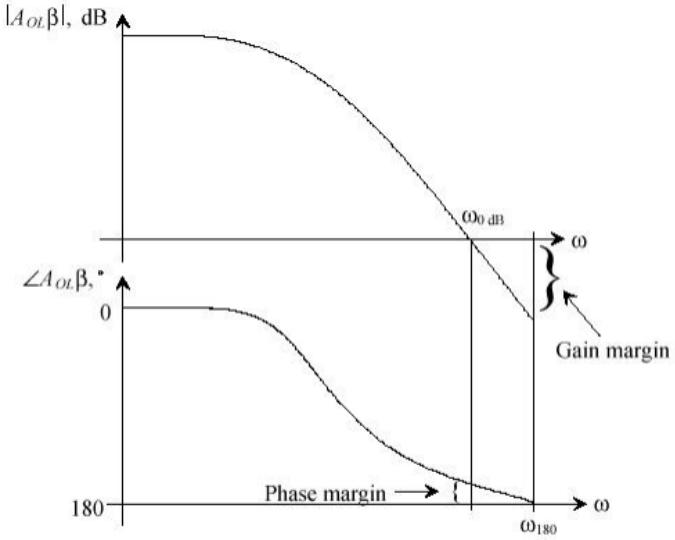

Figure 12. Gain margin and phase margin definitions (Blalock, 2001).

In order to calculate the margins, the Eq. 2 and Eq. 3 are used.

$$|K(j\omega_u)| = \frac{1}{|G(j\omega_u)|} \tag{2}$$

$$\angle K(j\omega_m) = -180° + \phi_m - \angle G(j\omega_m) \tag{3}$$

where $|K(j\omega_u)|$ is the control gain margin, $|G(j\omega_u)|$ is the plant gain margin, $\angle K(j\omega_m)$ is the controller phase margin, ϕ_m is the critical margin and $\angle G(j\omega_m)$ is the plant phase margin.

To calculate the PID parameters, the Eqs. 4, 5 and 6 are used.

$$K_P = \frac{1}{|G(j\omega_u)|\sqrt{1 + \left(\omega_u T_D - \frac{1}{\omega_u T_I}\right)^2}} \tag{4}$$

$$\omega_m T_D - \frac{1}{\omega_m T_I} = \tan\varphi \tag{5}$$

$$\varphi = -180^{\circ} + \phi_m - \angle G(j\omega_m) \tag{6}$$

where Kp is the proportional gain, TI the integrative part and TD the derivative part (Marques, 2009).

Once chosen the tuning method, it is possible to calculate the PID parameters. The function P1IZ estimated by "ident" toolkit of Matlab® is described in Eq. 7. The values Kp, Tp1 and Tz are shown below.

$$G(s) = Kp * \frac{1+Tz*s}{s(1+Tp1*s)} \tag{7}$$

with Kp = 0.0049201; Tp1 = 0.010331; Tz = 457.42

It is possible to observe the Bode diagram of the Eq. 7 in the Fig. 12. According to Fig. 12, there is a crossing line of -180° to achieve the gain margin, which appears to be infinite. Moreover, the critical phase margin is greater than or equal to 64°.

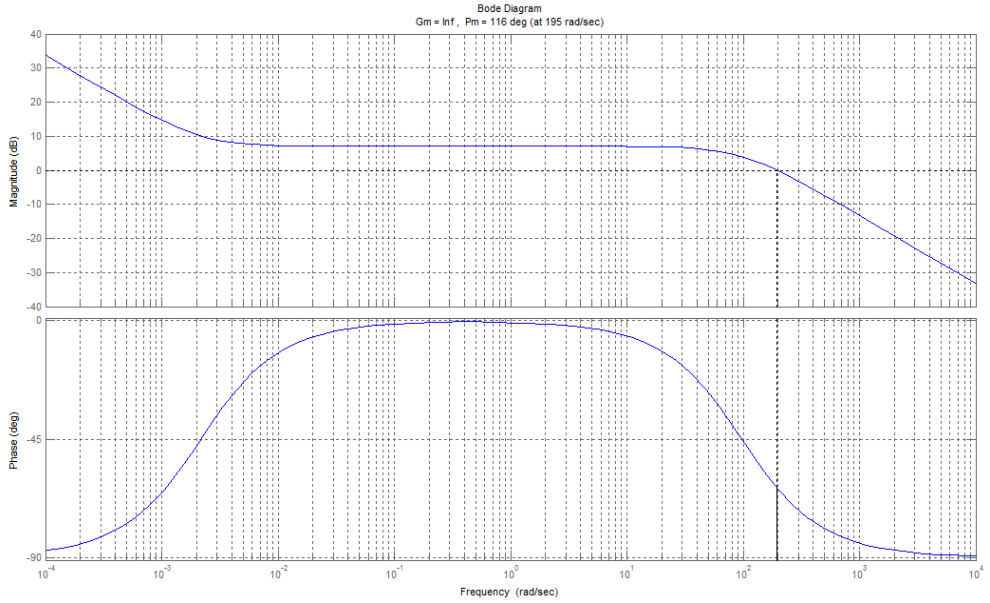

Figure 12. Bode diagrams for the uncontrolled system.

After determining the critical phase margin in the Bode diagram, one can apply the method to calculate the PID controller. For this, the PI controller was chosen, because it is the type used in 90% of industrial plants (Nicula, 2010). In order to obtain the optimum values, a table was constructed according to the values set for phase margin and gain margin and their parameters Kp, Ki and Kd, shown in Tab. 1.

Table 1. Matrix of parameters for phase margin, gain margin and parameters Kp, Ki and Kd.

Test	Gain margin	Phase margin	Kp	Ki	Kd
1	80	50	-0,0043	46,1146	0
2	80	64	0,1353	44,8275	0
3	80	90	0,3673	35,5455	0
4	70	64	0,0941	37,8155	0
5	140	64	0,3829	95,3515	0
6	300	64	1,0430	300,9167	0

According to the presented theory, for values whose phase margin is less than 64°, Kp was negative. Besides, keeping a certain gain margin by increasing the phase margin, Kp increased, while the Ki decreased. It was also noted that for the same phase margin, increasing the gain margin, both Kp and Ki increased.

4. RESULTS AND DISCUSSION

After performing the study about controller, ie to find the transfer function of the system, providing data on tuning of control and achieving the PID parameters, it should be tested to evaluate their efficiency. Firstly, it was evaluated the

behavior of curves generated using the software Matlab®, choosing as reference the entry step, because this will be the input value for the test system validation. The following Figures are displayed with their PID parameters, gain margin (GM) and phase margin (PM).

Figure 13 shows the result for a test Tab. 1. As expected, the system presented nearly 20% overshoot, low oscillatory behavior, since the parameters are negative. In this case, the control took 0.14 seconds to be achieved.

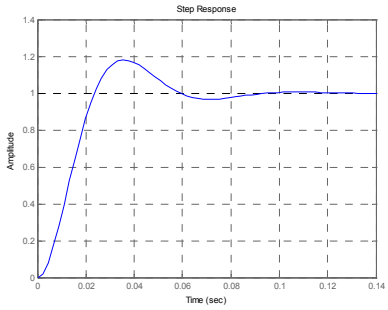

Figure 13. Test 1 step response with GM=80, PM=50, Kp=-0,0043, Ki=46,1146 and Kd=0.

Figure 14 shows the result for test 2 in Tab. 1. The system control also reached in 0.08 seconds, which proved effective. It is worth to mention the reduction of overshoot, less than 15%, and no error in steady state.

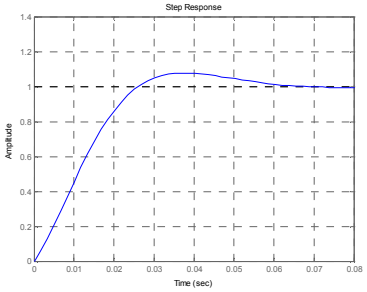

Figure 14. Test 2 step response with GM=80, PM=64, Kp=0,1353, Ki=44,8275 and Kd=0.

Figure 15 shows the result for test 3 of Tab. 1. The system has achieved control in 0.08 seconds. The control system has reached 0.08 seconds. In this case, improvement was obtained in relation to the settling time of the previous test. The error remains zero in steady state. However, it also increased the rise time.

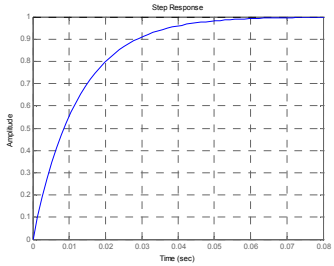

Figure 15. Test 3 step response with MG=80, MF=90, Kp=0,3673, Ki=35,5455 and Kd=0.

Figure 16 displays the result for test 4 of Tab. 1. The system achieved the control in 0.1 s. Thus, the settling time was less than the time of 0.08 seconds from the previous test 3. It had been noted an overshoot of approximately 7% and no error in steady state.

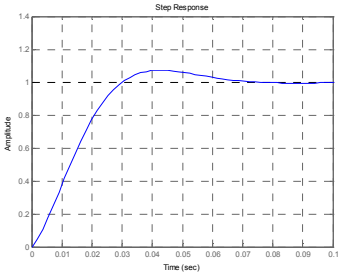

Figure 16. Test 4 step response Test 4 GM=70, PM=64, Kp=0,0941, Ki=37,8155 and Kd=0.

Figure 17 shows the result for the test 5 of Tab. 1. The control system has reached 0.035 s. Thus, the settling time was found lower compared to all previous tests, the overshoot is close to 12% was noted and no error in steady state.

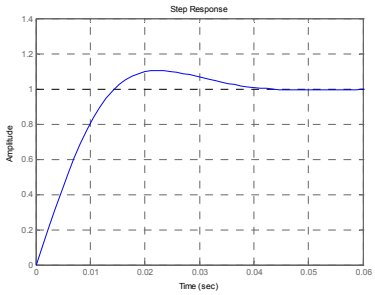

Figure 17. Test 5 step response with GM=140, PM=64, Kp=0,3829, Ki=95,3515 and Kd=0.

Figure 18 shows the result for the test 6 of Tab. 1. The system has achieved control in 0.06 seconds. It can be seen lower rise time, however, longer time to find stability in relation to the test of Fig. 17. It may be mentioned approximately 14% overshoot and no steady state error.

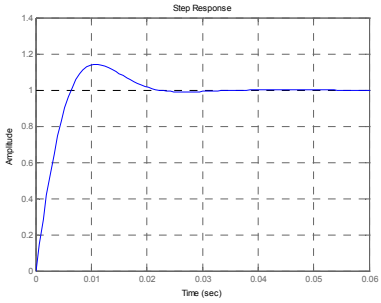

Figure 18. Test 6 step response with MG=300, MF=64, Kp=1,0430, Ki=300,9167 and Kd=0.

Among the six tests shown above, it was selected the fifth test, shown in Fig. 17 for application to the portable FHPP unit. This choice was made since it needed less time to find the control, overshoot close to 12%, no oscillation and rise times and lower stability compared to the earlier mentioned values. The data on Kp, Ki and Kd were applied in open loop controller card and the result is shown in Fig. 19. It can be seen that the system was successful in the proposed control.

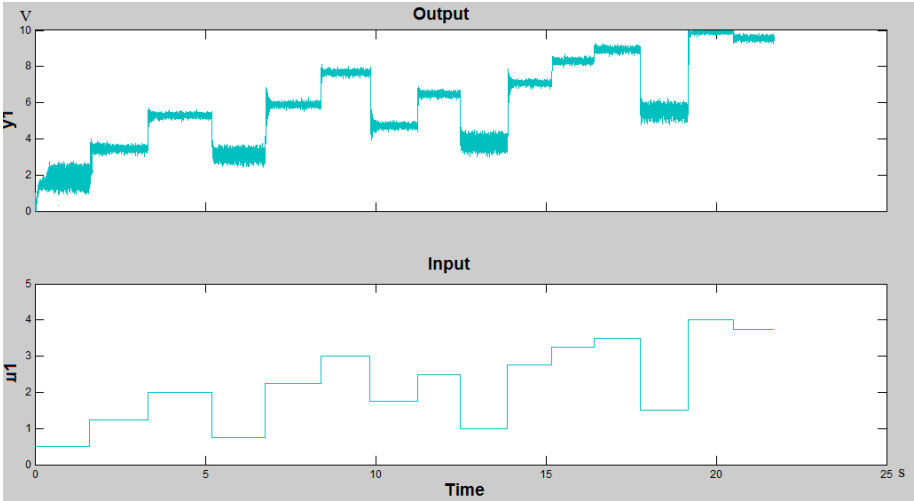

Figure 19. Graph of control applied to the system.

5. CONCLUSION

In this paper the rotation controller card parameters for a portable Friction Hydro Pillar Processing was optimized identifying the VT-HACD control card and the BODAC® program that is responsible for setting the control card. In addition, the study was carried out using graphics from previous tests performed in the equipment, analysis of the

transfer function and configuration of the optimal values of Kp, Ki and Kd. In the end, it could better use the better performance of the equipment during the tests.

It may be mentioned that the previous study about the control board VT-HACD provided greater knowledge about its functioning. The understanding of their position in the grid of the system, allowed choosing their mode of operation, ensuring more efficient in the control. In addition, since the VT-HACD card can be used as a command at another time in order to transmit signals to other components that demonstrates its versatility.

Graphical signal analysis of previously tests offered the needed information about the system behavior, since the relationship between rotation speed and force was known; also identify the observed equipment stalls. Thus, the analysis was made regarding the plant transfer function, using the toolkit "ident" of Matlab® software. Once having the transfer function, the calculation on the parameters of PID controller could be performed. For this, the method of frequency response was chosen, due to its ease in understanding and applying. After the calculus of Kp, Ki and Kd values, it was possible to conduct tests on the application of these parameters to rotation control of the equipment. It was possible to observe the influence of the variables during the tests.

6. ACKNOWLEDGEMENTS

The authors are grateful to FAPEMIG and FINEP/PETROBRAS for financial support.

7. REFERENCES

Andrews, R. E., "Underwater repair by friction stich welding, in Metals and Materials", p.796-797, 1990.

Blalock, B. J., "Analog IC Design", Mississipi, p. 116-123, 2001.

Rexroth Bosch Group, "VT-HACD-1 – Digital controller for electro mechanical and electrohydraulic drives", Germany, 2007, 262p.

Formoso, C. M., Jardim, M. P., Franco, V. L. D. S., Franco, S. D., Souza, V. B. J., "Desenvolvimento de um Sistema de Controle para uma Unidade de Processamento de Pinos por Atrito", 15º POSMEC – Pos-Graduation Symposio in Mechanical Enginnering, Mechanical Engineering School, Uberlandia Federal University, 2005.

Hwang, H. F., "Desenvolvimento, projeto, construção e teste de um cilindro de reparo por atrito portátil", in dissertation to Pos-Graduation Programme in Mechanical Enginnering, Mechanical Engineering School, Uberlandia Federal University, 2010.

Marques, J. P. P. T., "Modelação e controlo de conversor DC/AC para interligação de painéis fotovoltaicos à rede", in dessertation to Porto Engineering School, Porto, 2009.

Meyer, A., "Friction Hydro Pillar Processing", Dissertation an der Technischen Universität Braunschweig, Hamburg, 2002.

Nicholas, E. D., "Friction Hydro Pillar Processing", in 11th Annual North American Welding Research Conference7-9/11/1995.

Nicula, M. T., "Estudo, análise e simulação das técnicas de sintonia de controladores PID mais empregadas atualmente em plantas industriais", in monography to Graduation in Mechatronic Engineering, Mechanical Engineering School, Uberlandia Federal University, 2010.

Paula, C. F., Cunha, F. H. R., Ferreira, L. H. C., "Uma técnica aprimorada de sintonia analítica de controladores PID por resposta em frequência", em XVIII Automatica Brazilian Congress, Bonito, Mato Grosso do Sul, 2010.

Thomas, W. D. and Nicholas S. D., "Friction Forming", patent no. EP 0.602.072 B1, 1992.

Thomas, W. M. and Tempel-Smith, P., "Friction plug extrusion", GB 2.306.365, 1997.

Santos, G. M., Formoso, C. M., Hwang, H. F., Franco, V. L. D. S., Franco, S. D., "Controle e monitoramento de uma unidade de processamento de pinos por atrito para o reparo de dutos e tubulações de transporte de derivados de petróleo", VI CONEM – Mechanical Engineering Nacional Congress, Campina Grande, Paraíba, 2010.

Souza, R. J.,"Desenvolvimento, projeto e construção de um equipamento de reparo de trincas por atrito", in dissertation to Pos-Graduation Programme in Mechanical Engineering, Mechanical Engineering School, Uberlandia Federal University, 2006.

8. RESPONSIBILITY NOTICE

The authors are the only responsible for the printed material included in this paper.